

## RENAL CORTICAL IMAGING IN 35 PATIENTS: SUPERIOR QUALITY WITH $^{99m}\text{Tc}$ -DMSA

Derek Enlander, Paul M. Weber, and Leo V. dos Remedios  
Kaiser-Permanente Medical Center, Oakland, California

*The metal chelate 2,3-dimercaptosuccinic acid (DMSA) complexed with  $^{99m}\text{Tc}$  appears to be a superior and safe renal scintigraphic agent, regularly revealing corticomedullary morphology with either a multihole or a pinhole collimator. Fifty percent or more of administered dose is retained by the renal cortex at 1 hr—the highest proportion that has been reported for any  $^{99m}\text{Tc}$  complex. Scintiphotos of a variety of renal diseases and preliminary kinetic data are presented.*

With the remarkable renal scintigraphic agent,  $^{99m}\text{Tc}$ -caseidin, we obtained regularly, without special or lengthy procedures, image detail adequate to reveal the gross cortical and medullary morphology of normally functioning kidneys (1). Such definition became our principal criterion for judging the quality of renal scintigraphic agents. Unfortunately, this polypeptide casein derivative has not become readily available. High absorbed radiation dose per millicurie limits the image quality obtained with the radiomercurials and obviates their use for dynamic renal vascular flow studies (2). In an attempt to overcome these disadvantages, other  $^{99m}\text{Tc}$ -labeled scintigraphic agents have been evaluated:  $^{99m}\text{Tc}$ -diethyltriampentacetate (DTPA) (3),  $^{99m}\text{Tc}$ -Fe ascorbic acid (4–6), Renotec (7), and  $^{99m}\text{Tc}$ -penicillamine acetazolamide (TPAC) (7,8). In our experience and that of others, none revealed corticomedullary morphology with multihole collimators as did  $^{99m}\text{Tc}$ -caseidin (1,9).

During an antischistosomiasis campaign in the People's Republic of China, many cases of antimony poisoning occurred. The metal chelate 2,3-dimercaptosuccinic acid (DMSA), molecular weight 182, was

synthesized and used extensively in 1- to 2-gm doses as treatment for antimony, lead, or mercury poisoning. It was effective, and no significant clinical or laboratory adverse effects were noted (10). In mice the LD<sub>50</sub> of DMSA was reported to be about 2 gm/kg (10). DMSA complexed with SnCl<sub>2</sub> and  $^{99m}\text{TcO}_4^-$  has been shown in experimental animals to be an excellent renal cortical imaging agent (11). The usual human dose of 5 mCi of  $^{99m}\text{Tc}$ -DMSA contains less than 0.5 mg of DMSA, so the margin of safety appears to be large. We have demonstrated in a clinical trial in 35 patients that it is a safe and superior renal scintiphotographic agent, at least rivaling the excellent image quality of  $^{99m}\text{Tc}$ -caseidin. The high percentage of  $^{99m}\text{Tc}$ -DMSA retained in the renal cortex results in the high gamma flux and appropriate photopeak responsible for the superior resolution obtained. It is suitable for dynamic renal vascular flow studies.

### MATERIALS AND METHODS

**Preparation of the chelate complex.** The aqueous solution of DMSA (0.547 mg/ml) and SnCl<sub>2</sub> (0.19 mg/ml) at pH 2–3, obtained in a sterile, pyrogen-free kit,\* was thoroughly mixed with an equal volume of oxidant-free  $^{99m}\text{TcO}_4^-$  solution. After incubation at room temperature for 10–30 min, it was injected intravenously.

**Methods.** The hydrated patient lay prone under an Anger scintillation camera. For the kinetic phase,

Received Nov. 13, 1973; revision accepted Mar. 6, 1974.

For reprints contact: Paul M. Weber, 280 W. MacArthur Blvd., Oakland, Calif. 94611.

\* Medi-Physics, Inc., Kidney Scintigraphin®, Emeryville, Calif.

100  $\mu\text{Ci}$  of  $^{99\text{m}}\text{Tc}$ -DMSA was injected for renal localization. The 4000-hole or, if necessary, the low-energy diverging collimator was positioned over both kidneys and 5 mCi of  $^{99\text{m}}\text{Tc}$ -DMSA in less than 2-ml volume was injected as a bolus. When the persistence monitor scope began to show activity, the camera output was recorded on Polaroid film, hand-pulled at 3-sec intervals for eight scintiphotos, then at 9-sec intervals for eight additional scintiphotos, and simultaneously on  $10 \times 12$ -cm negative film by an Anger 80-lens sequential optical camera (12) at 2.4 sec/image.

In 21 patients, serial-timed blood samples were drawn for 60 min; in seven patients,  $^{125}\text{I}$  serum albumin was injected just before the  $^{99\text{m}}\text{Tc}$ -DMSA. Both plasma and whole blood were counted in a well counter with the window set at 130–150 keV for the  $^{99\text{m}}\text{Tc}$  energy. Iodine-125 plasma samples were counted at 15–45 keV after the  $^{99\text{m}}\text{Tc}$  had decayed. The fractional binding of  $^{99\text{m}}\text{Tc}$ -DMSA to red blood cells (RBC) was obtained by the following calculation:  $\{C_b - (C_p[1 - \text{hct}])\}/C_b$ , where  $C_b$  and  $C_p$  were net counts per minute per milliliter of whole blood and plasma, respectively, and hct the microhematocrit. Both  $^{125}\text{I}$  albumin plasma volume and  $^{99\text{m}}\text{Tc}$ -DMSA initial distribution volumes were calculated by relating appropriate calibrated standards to the zero-time extrapolate of the relevant plasma data. The fraction of administered dose excreted in the urine was determined by comparing  $^{99\text{m}}\text{Tc}$  activity in timed urine specimens with an appropriate standard. Fractional renal retention was calculated in eight patients. The whole-body distribution of  $^{99\text{m}}\text{Tc}$ -DMSA was studied in two patients with the whole-body scanner (13), renal activity being related to total-body activity by a digital computer system (14). In seven, the background-corrected kidney counting rate was compared with that in a renal phantom consisting of a solution of  $^{99\text{m}}\text{Tc}$  in plastic containers of appropriate size counted in renal geometry through Lucite absorbers.

Both patient and phantom data from the scintillation camera were digitized as time frames and a mini-computer system was used for data manipulation. One patient was studied before nephrectomy by both methods; kidney activity was quantified after nephrectomy with excellent agreement between the methods.

Scintiphotos of the kidneys were made at 1 hr after injection for 400k counts with the 15,000-hole high-resolution  $^{99\text{m}}\text{Tc}$  collimator. In addition, each kidney image was fully enlarged by means of the 5-mm pinhole collimator for 200k counts. In six patients, delayed scintiphotos were also made as late as 17 hr after injection. The thyroid area was

surveyed in 25 patients to evaluate the presence of free pertechnetate. A breath-holding technique intended to minimize the image-degrading effect of respiratory movement was evaluated.

#### SUBJECTS

All of the 35 subjects were outpatients in good general condition who had been referred for renal scintiphotography. Written informed consent was obtained in all cases, in accordance with Sec. 130.37 FDA regulations. All but two of the patients were adults. One 6-year-old boy was studied for possible congenital unilateral renal agenesis and a 15-year-old girl with Goodpasture's syndrome was studied. Excretory urograms of 25 patients were available; one patient had been studied with  $^{203}\text{Hg}$ -chlormerodrin and two with  $^{197}\text{Hg}$ -chlormerodrin. In four patients the serum creatinine was elevated (2.3–4.6 mg/dl); in all others whose serum creatinine was measured it was lower than 1.8 mg/dl. In 17 patients,  $^{131}\text{I}$ -hippuran renography was performed the day after the  $^{99\text{m}}\text{Tc}$ -DMSA study.

#### RESULTS

The early plasma disappearance curves of  $^{99\text{m}}\text{Tc}$ -DMSA in 15 of the 21 patients in whom this was measured appeared to fit a single exponential function, though in six an additional single blood sample drawn 14 hr after injection revealed that the plasma contained 6–9% of injected dose, confirming that in these cases the disappearance curve is more complex than the early data suggest. The mean half-times ( $t_{1/2}$ ) of early plasma  $^{99\text{m}}\text{Tc}$ -DMSA disappearance in these 15 patients was 62 min. Excluding the two patients with serum creatinine exceeding 2.0 mg/dl reduced this mean to 56 min (s.d.  $\pm 12$  min). In

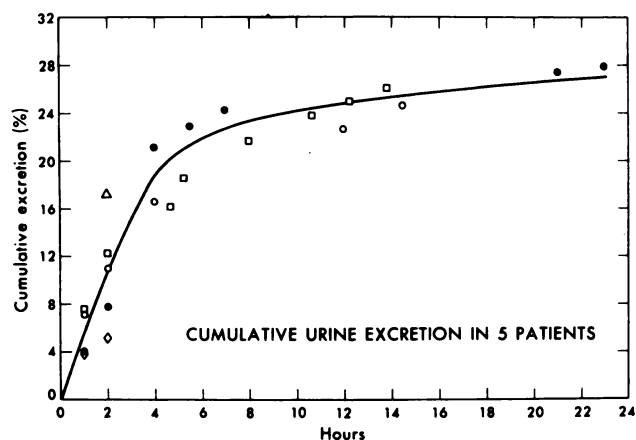
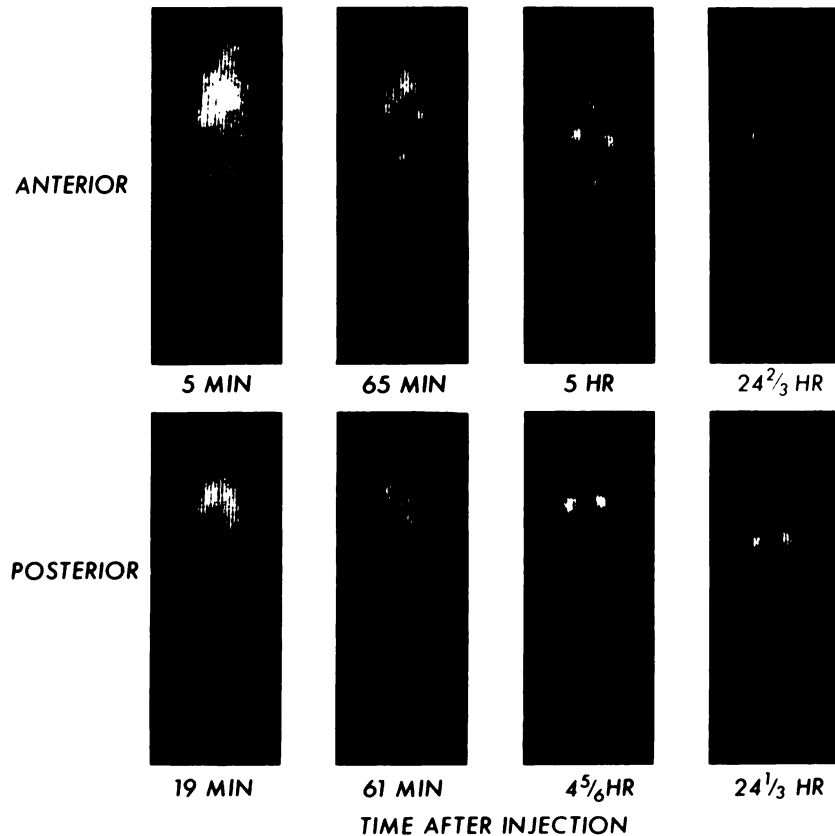


FIG. 1. Cumulative urinary  $^{99\text{m}}\text{Tc}$ -DMSA excretion in five patients.



**FIG. 2.** Whole-body scans at specified times after injection of  $^{99m}\text{Tc}$ -DMSA, in patient with poor renal function (creatinine clearance, 28 ml/min) (top) anterior and (bottom) posterior views. Shows initial blood-pool distribution followed by clearance, with rapid and progressive renal accumulation and excretion into bladder of small fraction. At 24 hr, trace of activity is noted in thyroid gland. This is only patient in whom any activity has been identified in thyroid gland at any time.

the other six, the curve represented a sum of exponentials that could not be solved from data accumulated only over the first 60 min.

In each of the seven patients who received  $^{125}\text{I}$  serum albumin, the initial plasma distribution volume from  $^{99m}\text{Tc}$ -DMSA slightly exceeded the respective  $^{125}\text{I}$  plasma volume with a mean difference of 12.5%.

Of the 20 patients studied for RBC binding, 12 showed none whereas in eight, from 1.5 to 10% (average 5%) of administered  $^{99m}\text{Tc}$  activity appeared bound to RBC during the 1 hr over which blood samples were obtained.

Cumulative urinary  $^{99m}\text{Tc}$ -DMSA excretion was plotted against time in five patients (Fig. 1). Four to 8% of the injected dose was excreted in the first hour; 8–17% cumulatively by 2 hr. In three patients from whom urine samples were collected for 14 hr or more, 26–29% of the administered dose was excreted by the end of that period.

In two patients, one without significant renal disease, the other with progressive renal failure and a creatinine clearance rate of only 28 ml/min, serial whole-body scanning after the administration of  $^{99m}\text{Tc}$ -DMSA showed rapid and progressive renal clearance of radioactivity from the blood (Fig. 2). Quantitative analysis of the data from these two

patients and from the phantom confirmed that whereas more than 70% of the injected dose was eventually found in the kidneys, approximately 50% was already there in 1 hr. At 24 hr, that remaining outside the kidneys appeared distributed throughout the body, presumably in the vascular space, with less than 0.1% apparent in the thyroid of one patient. There was no evidence of  $^{99m}\text{Tc}$  in the thyroid of the second of these two patients or of any other patient whose thyroid was imaged.

In all patients, each of the static scintiphotos obtained with the high-resolution collimator 1 hr after administration of  $^{99m}\text{Tc}$ -DMSA demonstrated a non-uniform distribution pattern of renal activity. This pattern was not invariably visualized when the 4000-hole collimator was used. Images taken later revealed increasing renal detail with decreasing background. The best scintiphotos were always those obtained late, about 13 hr after injection of a 5-mCi dose. At that time, about 7–8 min was required to accumulate 400k counts with the high-resolution collimator, imaging both kidneys simultaneously. When correction was made for physical decay, this appeared to indicate that about one and one-half times as much DMSA was in the kidney at 13 hr as after 1 hr when the required exposure time was about 2–4 min.



**FIG. 3.** Typical pattern in patient with normal renal function. High-resolution collimator late image reveals typical kidney fine structure (14 hr postinjection), seen even better in pinhole enlargements: (left) 400k, 363 sec; (middle) 200k, 377 sec; and (right) 200k, 442 sec.

When the 5-mm pinhole collimator was used and each kidney was enlarged to full crystal width, equivalent resolution was obtained with 200k counts in about 9 min, 15 hr after injection.

In one patient, scintiphotos taken 1 hr after injection during breath-holding only, at full expiration and then at full inspiration, showed that each kidney moved vertically about one-third of its length during deep respiration with some renal compression and slight rotation about the vertical axis. Each breath-held scintiphoto with 50k counts was of excellent quality whereas with deep breathing, as might have been expected, the renal morphology was blurred. With normal breathing, excellent definition was regularly obtained by means of the high-resolution collimator with 400k counts or by pinhole enlargement with 100k 1 hr after injection.

At no time did urinary radioactivity in the renal calices or pelves cause artifacts (7). Activity in the liver (7) or gastric mucosa (15) did not interfere with the renal image even in patients with poor creatinine clearance.

No adverse effect attributable to this study was noted in any patient.

From available clinical and laboratory data, the kidneys of 18 of these 35 patients were judged to be essentially normal (Fig. 3); the remaining 17 had a variety of abnormal renal findings. In four patients, the two kidneys differed markedly in size (Fig. 4).

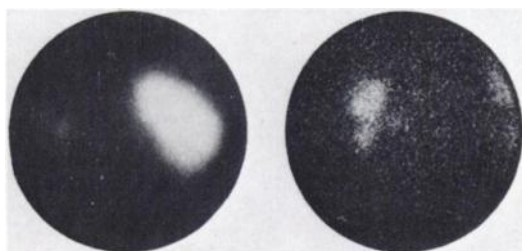
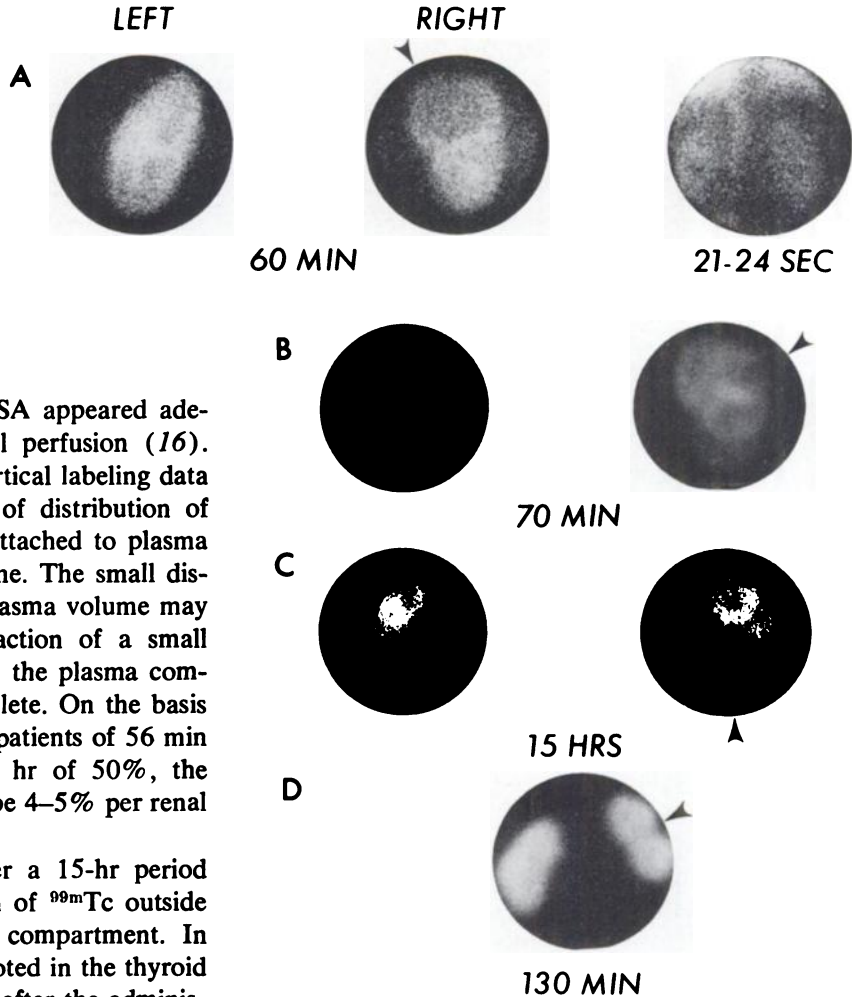


**FIG. 4.** Contracted left kidney secondary to renal artery embolus. Right corticomedullary structure not well seen at 1 hr with 4000-hole collimator. Anatomic detail of contracted left kidney well seen on pinhole enlargement. Contracted kidney was not visualized on excretory urograms or with chlormerodrin  $^{201}\text{Hg}$ .

In four others, one or more renal cortical lesions were identified (Fig. 5). In Patient 5A, a hypernephroma 6 cm in diam was found at nephrectomy at the upper pole of the right kidney in the site seen on the scintiphoto. In Patient 5B, the small cortical cyst demonstrated in the periphery of the right kidney by scintiphotography was also visualized by nephrotomography and arteriography and confirmed by needle aspiration. In Patient 5C, who had a history of recurrent urinary tract infections, retrograde pyelography confirmed hydronephrosis of the lower pole of the right kidney in the area visualized on the scintiphoto. Obstruction at the ureteropelvic junction was surgically corrected. Patient 5D, a 39-year-old man who had been polycythemic for 8 years, presented with the clinical findings typical of a right renal infarct. On the scintiphoto, a small, wedge-shaped defect was seen on the periphery of the right kidney in a site corresponding to a similar defect demonstrated on renal arteriograms. In nine patients (Fig. 6), the renal abnormalities were chiefly uneven or diminished cortical concentration or marked anatomic distortion due either to acute or chronic pyelonephritis or to hydronephrosis. Patient 6A had a history of bilateral chronic pyelonephritis. The scintiphotographic study was made during an acute exacerbation. Excretory urography could not be performed because the patient was allergic to radiopaque dyes. Patient 6B had marked hydronephrosis of the left kidney as demonstrated by excretory urography. The  $^{99\text{m}}\text{Tc}$ -DMSA dynamic study revealed reduced blood flow to the left kidney. The static images showed poor cortical labeling, worse along the medial margin of the kidney, suggesting renal pelvic dilatation. The hippuran study revealed the excretion pattern of obstruction on the left. A ureteropelvic junction band causing obstruction was resected. Patient 6C had hydronephrosis of the inferior two-thirds of the left kidney due to surgically confirmed ureteropelvic junction obstruction. In Patient 6D, the left kidney did not visualize on excretory urograms. Only a portion of the left kidney is included in the illustration here. At operation the hydronephrotic left kidney measured 25 cm in length.

**FIG. 5.** Solitary renal cortical lesions in four patients. Scintiphotos of Patient A, with hypernephroma, show large mass lesion at right upper pole. Three-second image from dynamic study demonstrates normal vascularity of this lesion. In Patient B, small cortical cyst is seen in right kidney. In Patient C, defect at right lower pole was proved to be hydronephrosis. Patient D had polycythemia vera; small right cortical lesion was renal infarct.



DISCUSSION

The 5-mCi bolus of <sup>99m</sup>Tc-DMSA appeared adequate for assessing regional renal perfusion (16). Blood disappearance and renal cortical labeling data suggest that initially the volume of distribution of <sup>99m</sup>Tc-DMSA which is probably attached to plasma proteins (11) is the plasma volume. The small disparity between this and the <sup>125</sup>I plasma volume may have been caused by renal extraction of a small fraction of the <sup>99m</sup>Tc-DMSA from the plasma compartment before mixing was complete. On the basis of both the plasma t<sub>1/2</sub> in normal patients of 56 min and the renal accumulation in 1 hr of 50%, the extraction fraction is estimated to be 4–5% per renal passage.

Whole-body serial imaging over a 15-hr period revealed little or no concentration of <sup>99m</sup>Tc outside the kidney, bladder, or vascular compartment. In particular, no concentration was noted in the thyroid gland except in one patient, 24 hr after the administered dose. This would indicate that the dissociation of <sup>99m</sup>Tc-DMSA does not occur until late and even then is small.

The definition and resolution of the <sup>99m</sup>Tc-DMSA images were slightly better than those we previously obtained with <sup>99m</sup>Tc-caseidin (1) and were clearly superior to those with Renotec (7). The improvement appears to be the result of several factors. The <sup>99m</sup>Tc-DMSA seems to be largely bound to plasma proteins (11); this prevents significant filtration

through the glomeruli so that the renal pelvic urine contains too little activity to cause artifacts. About 4–5% of <sup>99m</sup>Tc-DMSA in the renal blood is continuously extracted as it passes through the kidneys. Quantitative data indicate that probably about 50% of the administered dose is firmly bound to the kidneys in 1 hr. Table 1 shows that the retention of this fraction of the dose was not equaled with any <sup>99m</sup>Tc-labeled renal imaging agent reported heretofore.

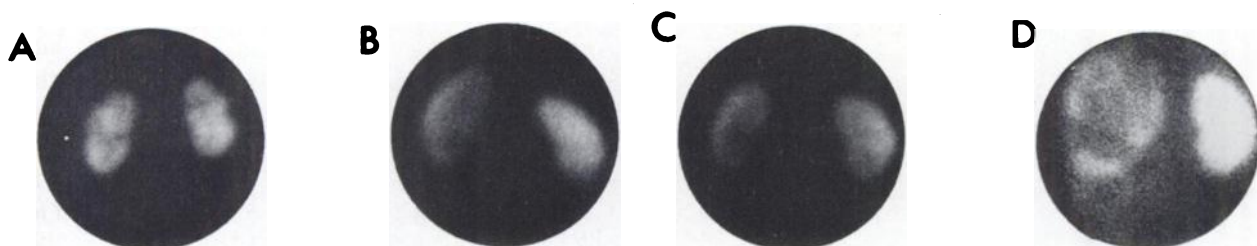


**FIG. 6.** Scintiphoto A is pattern typically seen with bilateral chronic pyelonephritis. B, C, D, and Fig. 5C represent spectrum of

image patterns seen with hydronephrosis. A, 16 hr; B, 6 hr; C, 16 hr; and D, 17 hr.

**TABLE 1. RENAL RETENTION OF VARIOUS  $^{99m}\text{Tc}$ -LABELED SUBSTANCES**

$^{99m}\text{Tc}$ -labeled complex	% of dose retained in 2 kidneys in 1 hr	Animal studied	Reference
DTPA	<0.5	Mouse	17
Renotec	2	Mouse	17
Fe-ascorbate	9	Rat	9
Caseidin	24	Rat	9
Glucoheptonate	22	?	18
DMSA	54	Rat	10
DMSA	$\geq 50$	Man	This paper
$^{203}\text{Hg}$ -chlormerodrin	65	Rat	9

The cortical morphology of the normal kidney appears in the images as a thin peripheral rim of  $^{99m}\text{Tc}$ -DMSA activity which merges with a central network of activity enclosing 4–8 relatively "cold" areas (1,5,11). This reticular pattern probably results from the high activity in the cortical columns of Bertin, extending into the "colder" medulla, and separating it into several irregular pyramidal structures which, when viewed from the base, appear polygonal. Normal variations of this new renal cortical image must be learned to avoid misinterpreting normal structures as renal defects.

All "pure"  $^{99m}\text{Tc}$ -DTPA chelates are filtered (3,17) by the glomerulus and less than 0.5% is retained in the renal cortex (18); this small quantity cannot be expected to give good static renal cortical images. When we have used Renotec, a mixture of  $^{99m}\text{Tc}$ -DTPA and  $^{99m}\text{Tc}$ -Fe ascorbate, renal pelvic artifacts have distorted the cortical image (7) and gamma flux is disturbingly low (18). Technetium-99m-caseidin gave images equivalent to  $^{99m}\text{Tc}$ -DMSA but its concentration in the renal cortex is slightly less; furthermore, because it is a hydrolysate of casein, it may possibly be allergenic. The complexes of  $^{99m}\text{Tc}$ -penicillamine (8) hold promise as renal cortical imaging agents, but appear to be metabolized fairly rapidly (8), and published scintiphotos do not reveal the cortical morphology. Very recently,  $^{99m}\text{Tc}$ -glucoheptonate (19) has been introduced; but since only 22% is retained in the kidney at 1 hr. this agent probably will prove to be less efficient than  $^{99m}\text{Tc}$ -DMSA.

**Radiation dosimetry.** The absorbed radiation dose per millicurie administered was calculated to be 1.4 rads to the kidney and 0.015 rad to the whole body.

#### ACKNOWLEDGMENT

Supported in part by Grant 111-9623, Kaiser Foundation Research Institute.

#### REFERENCES

1. LIN MS, WEBER PM, WINCHELL HS, et al: Renal imaging in humans with the technetium-labeled polypeptide caseidin. *J Nucl Med* 13: 517–521, 1972
2. MCAFEE JG: Problems in evaluating the radiation dose for radionuclides excreted by the kidneys. In *Medical Radionuclides: Radiation Dose and Effects*. Cloutier RJ, Edwards CL, Snyder WS, eds, Symposium Series 20, CONF-691212, Oak Ridge, Tenn, USAEC TID, 1970, pp 271–294
3. HAUSER W, ATKINS HL, NELSON KG, et al: Technetium-99m DTPA: a new radiopharmaceutical for brain and kidney scanning. *Radiology* 94: 679–684, 1970
4. HARPER PV, LATHROP KA, HINN GM, et al: Technetium-99m—iron complex. In *Radioactive Pharmaceuticals*. Andrews GA, Kniseley RM, Wagner, HN, eds, Symposium Series 6, CONF-651111, Springfield, Va, National Bureau of Standards, 1966, pp 347–351
5. BLUM AS, POPPITI RJ: Detailed kidney structure with  $^{99m}\text{Tc}$ -Fe and pinhole Anger camera. *J Nucl Med* 12: 418, 1971
6. WINSTON MA, HALPERN SE, WEISS ER, et al: A critical evaluation of  $^{99m}\text{Tc}$ -Fe-ascorbic acid complex as a renal scanning agent. *J Nucl Med* 12: 171–175, 1971
7. HALPERN SE, TUBIS M, GOLDEN M, et al:  $^{99m}\text{Tc}$ -TPAC, a new renal scanning agent. II. Evaluation in humans. *J Nucl Med* 13: 723–728, 1972
8. HALPERN S, TUBIS M, ENDOW J, et al:  $^{99m}\text{Tc}$ -penicillamine-acetazolamide complex, a new renal scanning agent. *J Nucl Med* 13: 45–50, 1972
9. WINCHELL HS, LIN MS, SHIPLEY B, et al: Localization of polypeptide caseidin in the renal cortex: A new radioisotope carrier for renal studies. *J Nucl Med* 12: 678–682, 1971
10. WANG SC, TING KS, WU CC: Chelating therapy with NA-DMS in occupational lead and mercury intoxications. *Chinese Med J* 84: 437–439, 1965
11. LIN TH, KHENTIGAN A, WINCHELL HS: A  $^{99m}\text{Tc}$ -chelate substitute for organoradiomercurial renal agents. *J Nucl Med* 15: 34–35, 1974
12. ANGER HO: *Eighty-Lens Optical Camera for Recording Dynamic Studies with Scintillation Camera*. University of California Radiation Laboratory Report No. UCRL-20699, Berkeley, Calif.
13. ANGER HO: Whole-body scanner mark II. *J Nucl Med* 7: 331–332, 1966
14. BUDINGER TF, GULLBERG GT, NOHR ML, et al: *Quantitative Sequential Imaging of Radionuclide Distribution Using the Whole-Body Scanner and the Gamma Camera: Absolute Accuracy and Aspects of Three-Dimensional Reconstruction*. Lawrence Berkeley Laboratory Report No. 6301, University of California Berkeley. Gesellschaft für Nuclearmedizin, Athens, Greece, September 1973
15. MCKUSICK KA, MALMUD LS, KIRCHNER PT, et al: An interesting artifact in radionuclide imaging of the kidneys. *J Nucl Med* 14: 113–114, 1973
16. POWELL MR, ANGER HO: Blood flow visualization with the scintillation camera. *J Nucl Med* 7: 729–732, 1966
17. BIANCHI C: Measurement of the glomerular filtration rate. In *Progress in Nuclear Medicine. Evaluation of Renal Function and Disease with Radionuclides*, vol 2, Blau-



fox MD, ed, Baltimore, University Park Press, 1972, pp 21-53

18. KONIKOWSKI T, GLENN HJ, HAYNIE TP: Renal clearance and brain tumor localization in mice of  $^{99m}\text{Tc}$  com-

pounds of (Sn)DTPA, (iron-ascorbic acid) DTPA, and iron-ascorbic acid. *J Nucl Med* 13: 834-842, 1972

19. New England Nuclear Package Insert. NEN  $^{99m}\text{Tc}$  stannous-glucoheptonate. North Billerica, Mass

### Accepted Articles To Appear in Upcoming Issues

- Comparison of  $^{99m}\text{Tc}$ -Polyphosphate and  $^{18}\text{F}$ . I. Kinetics. Accepted 4/11/74.  
G. T. Krishnamurthy, P. B. Thomas, M. Tubis, J. S. Endow, J. H. Pritchard, and W. H. Blahd
- Comparison of  $^{99m}\text{Tc}$ -Polyphosphate and  $^{18}\text{F}$ . II. Imaging. Accepted 4/11/74.  
G. T. Krishnamurthy, C. F. Walsh, L. E. Shoop, H. G. Berger, and W. H. Blahd
- $^{203}\text{Pb}$  for Bone Scanning (Letter to the Editor). Accepted 4/16/74.  
I. B. Syed
- The Author's Reply. Accepted 4/16/74.  
D. V. Rao
- Analog Image Processing in Two Dimensions by Omnidirectional Scanning. Accepted 4/18/74.  
N. Nohara, T. Tomitani, and E. Tanaka
- Visualization of Placental Abruption by Blood Pool Scanning (Case Report). Accepted 4/18/74.  
P. H. Weiss and J. D. Strong
- Radiation Exposure to the Family of Radioactive Patients (Concise Communication). Accepted 4/29/74.  
J. C. Harbert and N. Wells
- Determination of Impurity Activities in Fission Product Generator Eluate (Concise Communication). Accepted 4/29/74.  
D. W. Anderson, D. E. Raeside, and V. J. Ficken
- Hepatic Cavernous Hemangioma Presenting as an "Avascular Mass" in a Newborn (Case Report). Accepted 4/29/74.  
W. Beal, J. S. Soin, and J. A. Burdine
- $^{99m}\text{Tc}$ -Polyphosphate Concentration in a Neuroblastoma (Case Report). Accepted 4/29/74.  
P. M. Fitzer
- Arthroscintigraphy of Knee (Letter to the Editor). Accepted 4/29/74.  
R. Arkless
- The Authors' Reply. Accepted 4/29/74.  
R. V. Pozderac and A. E. Good
- Another Means of Diagnosing Synovial Cyst Dissection (Letter to the Editor). Accepted 4/29/74.  
M. A. Winston and J. H. Pritchard
- $^{125}\text{I}$ -IHSA versus  $^{109}\text{Yb}$ -DTPA for Cisternography (Letter to the Editor). Accepted 4/29/74.  
P. M. Ronai
- The Author's Reply. Accepted 4/29/74.  
J. C. Harbert
- Angioscintigraphy versus Portable Probe Technique as a Routine Diagnostic Aid for Cerebral Death (Letter to the Editor). Accepted 4/29/74.  
P. Braunstein, I. I. Kricheff, J. Korein, and R. Chandra
- The Authors' Reply. Accepted 4/29/74.  
S. Nordlander, P.-E. Wiklund, and P.-E. Åsard
- Radionuclide Venography (Letter to the Editor). Accepted 4/29/74.  
U. Y. Ryo
- The Authors' Reply. Accepted 4/29/74.  
R. E. Henkin, J. S. T. Yao, J. L. Quinn III, and J. J. Bergen
- Clinical Comparison of the Kinetics of  $^{99m}\text{Tc}$ -Labeled Polyphosphate. Accepted 5/9/74.  
G. T. Krishnamurthy, M. Tubis, J. S. Endow, V. Singhi, C. F. Walsh, and W. H. Blahd
- Comparison of the Metabolism of Iron-Labeled Transferrin (Fe-TF) and Indium-Labeled Transferrin (In-TF) by the Erythropoietic Marrow. Accepted 5/9/74.  
P. A. McIntyre, S. M. Larson, E. A. Eikman, M. Colman, U. Scheffel, and B. Hodkinson
- A Novel  $^{125}\text{I}$ -Labeling Reagent. XIII. Synthesis and Loading Dose. Accepted 5/9/74.  
R. M. Lambrecht, H. Atkins, H. Elias, J. S. Fowler, S. S. Lin, and A. P. Wolf
- Continuous Radionuclide Generation. I. Production and Evaluation of a  $^{81m}\text{Kr}$  Minigenerator. Accepted 5/9/74.  
L. G. Colombetti, L. W. Mayron, E. Kaplan, W. E. Barnes, A. M. Friedman, and J. E. Gindler
- Continuous Radionuclide Generation. II. Scintigraphic Definition of Capillary Exchange by Rapid Decay of  $^{81m}\text{Kr}$  and Its Applications. Accepted 5/9/74.  
E. Kaplan, L. W. Mayron, W. E. Barnes, L. G. Colombetti, A. M. Friedman, and J. E. Gindler
- Detection of Small Bone Abscesses with a High-Resolution Cadmium Telluride Probe (Concise Communication). Accepted 5/9/74.  
D. A. Garcia, G. Entine, and D. E. Tow
- Difference in Choroid Plexus Concentration of Perchnetate Produced by Varying Time of Perchlorate Administration and Brain Imaging. Accepted 5/10/74.  
N. P. Alazraki, R. L. Littenberg, S. Hurwitz, R. R. Quinto, S. E. Halpern, and W. L. Ashburn
- Long-Distance Transmission of Analog Gamma Camera Signals (Concise Communication). Accepted 5/10/74.  
D. J. Dowsett and K. Roberts
- The "Luxury-Perfusion Syndrome" following a Cerebrovascular Accident Demonstrated by Radionuclide Angiography (Case Report). Accepted 5/10/74.  
R. M. Snow and J. W. Keyes, Jr.
- Calcium, Phosphorus, and  $^{99m}\text{Tc}$  "Uptake" (Letter to the Editor). Accepted 5/10/74.  
E. B. Silberstein
- Pseudotumors in Acute Hepatitis (Case Report). Accepted 5/16/74.  
M. A. Winston
- Polyphosphate Bone Scans,  $^{32}\text{P}$ , and Adenocarcinoma of the Thyroid (Case Report). Accepted 5/16/74.  
L. Kiinger
- A Method of Tomographic Imaging using a Multiple Pinhole-Coded Aperture (Preliminary Note). Accepted 5/16/74.  
L.-T. Chang, S. N. Kaplan, B. Macdonald, V. Perez-Mendez, and L. Shiraishi
- A Rapid and Accurate Method for Sizing Radiocolloids. Accepted 5/20/74.  
M. A. Davis, A. G. Jones, and H. Trindade
- Partial Calcium Measurements by In Vitro Neutron Activation Analysis Comparisons with X-Ray Photodensitometry of the Radius. Accepted 5/22/74.  
J. E. Harrison, K. G. McNeill, H. E. Meema, S. Fenton, D. G. Oreopoulos, and W. C. Sturtridge
- Successful Modifications for Pancreatic Imaging. Accepted 5/22/74.  
S. Chandra and J. A. Prezio
- Rapid Hepatic Turnover of Radioactive Human Serum Albumin-Sensitized Dogs. Accepted 5/22/74.  
K. Kitani and G. V. Taplin
- Nonspecificity of the Radiocolloid Hepatic "Hotspot" for Superior Vena Caval Obstruction (Case Report). Accepted 5/22/74.  
R. S. Hattner and D. M. Shams
- Scintigraphic Demonstration of Bile Leakage Utilizing  $^{125}\text{I}$ -Rose Bengal (Case Report). Accepted 5/22/74.  
S. N. Wiener and M. Vyas
- Applications of Hippurate Kinetic Models (Letter to the Editor). Accepted 5/22/74.  
L. Reese
- The Authors' Reply. Accepted 5/22/74.  
J. A. DeGrazia, P. O. Scheibe, P. E. Jackson, Z. J. Lucas, W. R. Fair, J. M. Vogel, and L. J. Blumin
- $^{109}\text{Er}$ : An "Ideal" Radionuclide for Imaging with Pressurized Multi-wire Proportional Gamma Cameras (Concise Communication). Accepted 5/22/74.  
D. V. Rao, P. N. Goodwin, and F. L. Khalil
- Dosimetry of Copper Radionuclides (Concise Communication). Accepted 5/22/74.  
L. R. Chervu and I. Sternlieb
- Effect of a Scattering Medium on Gamma-Ray Imaging. Accepted 5/23/74.  
J. C. Ehrhardt, L. W. Oberley, and S. C. Lensink
- Feasibility of Consecutive-Day Schilling Tests. Accepted 5/29/74.  
G. M. Grames, R. Reisinger, C. Jansen, and R. Herber
- Radionuclide Angiography with  $^{99m}\text{Tc}$ -Labeled Red Blood Cells for the Detection of Aortic Aneurysm (Concise Communication). Accepted 5/29/74.  
U. Y. Ryo, J. I. Lee, H. Zarnow, M. P. Schwartz, and S. Pinsky
- Pseudoparasagittal Masses Caused by Displacement of the Falx and Superior Sagittal Sinus (Case Report). Accepted 5/29/74.  
S. K. Teplick, R. L. Van Heertum, R. E. Clark, and A. P. Carter
- A Brain Tumor Detected by the Nuclear Cerebral Angiogram (Case Report). Accepted 5/29/74.  
J. Rockett, M. Ray, M. Moinuddin, and C. Gardner
- Albumin-Loading Effect: A Pitfall in Saline Paper Analysis of  $^{99m}\text{Tc}$ -Albumin (Concise Communication). Accepted 5/30/74.  
M. S. Lin, S. L. Kruse, D. A. Goodwin, and J. P. Kriss
- Accuracy of Radionuclide Cerebral Angiograms in the Detection of Cerebral Arteriovenous Malformations. Accepted 6/4/74.  
J. W. Tyson, L. R. Witherspoon, R. H. Wilkinson, Jr., and J. K. Goodrich
- Resolution Capability of a Multiprobe System for Determining Regional Lung Perfusion with  $^{133}\text{Xe}$ . Accepted 6/4/74.  
M. Ramanathan and J. E. Wilson III
- Comparison of  $^{86}\text{Rb}$  and Microsphere Estimates of Left Ventricular Blood-Flow Distribution. Accepted 6/4/74.  
L. Becker, R. Ferreira, and M. Thomas
- Radionuclide Tomographic Image Reconstruction Using Fourier Transform Techniques. Accepted 6/4/74.  
D. B. Kay, J. W. Keyes, Jr., and W. Simon
- $^{133}\text{Xe}$  Ventilation Scanning Immediately following  $^{99m}\text{Tc}$  Perfusion Scan. Accepted 6/4/74.  
J. G. Jacobstein
- "Kit" Preparation of Radioiodinated Autologous Fibrinogen using  $^{125}\text{I}$ -Monochloride. Accepted 6/4/74.  
P. Hagan, M. D. Loberg, B. A. Rhodes, K. Harrison, and M. D. Cooper

Continued on page 813